intra-RTN inhibition is sufficient to produce thalamic hypersynchrony.

The powerful effects of β_3 ablation could be explained by the dependence of $GABA_A$ responses in RTN neurons on relatively few receptor isoforms (*11*). $GABA_A$ receptor function is less impaired in hippocampal neurons of β_3 knockouts (*21*), which may reflect a lower dependence on this β subunit (*11*). The shortening of IPSC duration in β_3 knockouts potentially relates IPSC properties to neural circuit activity in the thalamus and may show how the specific functional deletion of intra-RTN connections affects phasic oscillations (*7, 8*). The role of intra-RTN connections in thalamic oscillations is controversial. These connections might either facilitate (*22*) or dampen oscillations (*7, 9, 23*). Our results, showing highly synchronous oscillations in animals lacking functional $GABA_A$ receptors in RTN, indicate that intra-RTN inhibition desynchronizes thalamic activity. Further, these data show how inactivation of a postsynaptic receptor gene can result in functional deletion of a specific neuroanatomical circuit and provide information regarding mechanisms of human disease (*13*).

References and Notes

1. M. Steriade and R. R. Llinas, *Physiol. Rev.* **68**, 649 (1988).
2. M. Steriade, D. A. McCormick, T. J. Sejnowski, *Science* **262**, 679 (1993).
3. J. R. Huguenard and D. A. Prince, *J. Neurosci.* **14**, 5485 (1994).
4. M. von Krosigk, T. Bal, D. A. McCormick, *Science* **261**, 361 (1993).
5. R. W. Warren, A. Agmon, E. G. Jones, *J. Neurophysiol.* **72**, 1993 (1994).
6. M. E. Scheibel and A. B. Scheibel, *Brain Res.* **1**, 43 (1966); E. G. Jones, *J. Comp. Neurol.* **162**, 285 (1975); C. L. Cox, J. R. Huguenard, D. A. Prince, *ibid.* **366**, 416 (1996); D. Pinault, Y. Smith, M. Deschênes, *J. Neurosci.* **17**, 3215 (1997).
7. J. R. Huguenard and D. A. Prince, *J. Neurophysiol.* **71**, 2576 (1994).
8. U. Kim, M. V. Sanchez-Vives, D. A. McCormick, *Science* **278**, 130 (1997).
9. M. V. Sanchez-Vives, T. Bal, D. A. McCormick, *J. Neurosci.* **17**, 8894 (1997).
10. S. J. Zhang, J. R. Huguenard, D. A. Prince, *J. Neurophysiol.* **78**, 2280 (1997).
11. W. Wisden, D. J. Laurie, H. Monyer, P. H. Seeburg, *J. Neurosci.* **12**, 1040 (1992). Peak expression levels of β_3 subunit are in hippocampus, cerebellum, pyriform cortex, and olfactory bulb. In thalamus, β_3 is restricted to RTN and midline nuclei.
12. R. L. Macdonald and R. W. Olsen, *Annu. Rev. Neurosci.* **17**, 569 (1994).
13. G. E. Homanics *et al.*, *Proc. Natl. Acad. Sci. U.S.A.* **94**, 4143 (1997); T. M. DeLorey *et al.*, *J. Neurosci.* **18**, 8505 (1998).
14. Electroencephalographic oscillations during sleep and absence epilepsy result from synchronous activity in the cerebral cortex. They depend on synaptic interactions among neurons of RTN, thalamocortical relay nuclei, and cerebral cortex [reviewed in (*2*)].
15. Experiments were performed in accordance with procedures established by the Administrative Panel on Laboratory Animal Care at Stanford University. Briefly, adult mice, ranging in age from postnatal day 21 (P21) through P94 were anesthetized with pentobarbital (55 mg/kg body weight). We obtained 200-μm horizontal slices, using chilled slicing solution [115 mM choline-chloride, 26 mM $NaHCO_3$, 10 mM glucose, 2.5 mM KCl, 1.25 mM NaH_2PO_4, 10 mM $MgSO_4$, and 0.5 mM $CaCl_2$ (290 mosm)], and then incubated the slices at 32C in physiological saline (2 mM $CaCl_2$, 2 mM $MgSO_4$, and 126 mM NaCl) for 1 hour. Recordings (L/M-EPC7, Darmstadt, Germany) were at room temperature (21° to 23°C) with perfusion of physiological saline (2 ml/min). The holding potential was −60 mV, and with $E_{Cl} \approx 0$ mV, IPSCs were inward events. RTN and VB neurons were identified and recorded in a chamber affixed to the stage of an upright microscope (Leitz Laborlux). Electrodes were filled with pipette solution [135 mM CsCl, 5 mM QX314, 2 mM $MgCl_2$, 10 mM EGTA, 10 mM Hepes (pH 7.3)] and had resistances of 2.0 to 3.3 megohms. IPSCs were filtered at 1 kHz and stored on VCR tape (Neuro-corder, Cygnus Technology, Delaware Water Gap, PA). Spontaneous events were digitized with Axotape, version 2 (Axon Instruments), then were sorted and analyzed using Detector (version 4.8, J. R. Huguenard), Scan (J. R. Dempster), and Metatape (version 14.0, J. R. Huguenard). Unless otherwise noted, all statistical values indicate results of Student's *t* test.
16. Iontotropic glutamate receptors were blocked via bath application of 6,7-dinitroquinoxaline-2,3-dione (20 μM DNQX) [Research Biochemicals International (RBI), Natick, MA] and (+/–)-2-amino-5-phosphonopentanoic acid (100 μM AP-5) (RBI). Inhibitory $GABA_B$ receptors were blocked with CsCl and QX-314 (5 mM) in the internal pipette solution. IPSC decay was quantified by fitting double exponentials to averaged sIPSCs (>50 events from each neuron). Weighted decay time constants ($\tau_{D,W}$), derived from these fitted curves, provide a simple means to quantify IPSC duration [M. V. Jones and G. L. Westbrook, *J. Neurosci.* **17**, 7626 (1997)].
17. eIPSCs were obtained by stimulating RTN with a bipolar tungsten electrode. Stimuli were 1.5 times threshold (1.5 to 4 mA; 80 to 200 μs).
18. Extracellular multiunit recordings were performed as previously described using tungsten electrodes placed in RTN and the VB complex [D. Ulrich and J. R. Huguenard, *Neuron* **15**, 909 (1995)]. Extracellular stimulus (20 to 60 V, 30 μs, 0.05 Hz) to the internal capsule evoked oscillatory responses. Signals were band-pass filtered (30 Hz to 3 kHz) and recorded at 10 kHz, using Axotape, version 2.0 (Axon Instruments, Foster City, CA). Field responses were filtered between 3 and 100 Hz. Oscillations were blocked by 10 μM bicuculline methiodide (BMI) or 50 μM picrotoxin.
19. P. König, *J. Neurosci. Methods* **54**, 31 (1994). A modified Gabor function measured distinct autocorrelogram components: a central peak (CP), an exponentially decaying cosine function (Osc), and an offset (Off). Oscillatory index was then Osc/(CP + Osc + Off) × 100%.
20. BMI (n = 18 slices) or picrotoxin (n = 4) enhanced oscillatory output when applied locally (500 μM via pressure application pipette) to RTN (137 ± 13% of control, $P < 0.0001$), but not VB (13 ± 2% of control, $P < 0.01$).
21. M. D. Krasowki, C. E. Rick, N. L. Harrison, L. L. Firestone, G. E. Homanics, *Neurosci. Lett.* **240**, 81 (1998).
22. M. Steriade, L. Domich, G. Oakson, M. Deschênes, *J. Neurophysiol.* **57**, 260 (1987); A. Destexhe, D. Contreras, T. J. Sejnowski, M. Steriade, *ibid.* **72**, 803 (1994).
23. G. Ahlsén and S. Lindström, *Brain Res.* **236**, 482 (1982); D. Ulrich and J. R. Huguenard, *J. Neurophysiol.* **78**, 1748 (1997).

24. We thank C. Ferguson and J. Steinmiller for technical assistance and L. L. Firestone, R. W. Olsen, P. S. Buckmaster, N. A. Lambert, and D. A. Prince for support, encouragement, and helpful comments. Supported by NIH grants NS06477, NS34774, AA10422, and GM52035; the Pimley Research Fund; and the University Anesthesiology and Critical Care Medicine Foundation. Additional information may be obtained at http://tonto.stanford.edu/~john.

16 September 1998; accepted 10 December 1998

Prevention of Constitutive TNF Receptor 1 Signaling by Silencer of Death Domains

Yingping Jiang, John D. Woronicz, Wei Liu, David V. Goeddel*

Tumor necrosis factor receptor type 1 (TNF-R1) contains a cytoplasmic death domain that is required for the signaling of TNF activities such as apoptosis and nuclear factor kappa B (NF-κB) activation. Normally, these signals are generated only after TNF-induced receptor aggregation. However, TNF-R1 self-associates and signals independently of ligand when overexpressed. This apparent paradox may be explained by silencer of death domains (SODD), a widely expressed ~60-kilodalton protein that was found to be associated with the death domain of TNF-R1. TNF treatment released SODD from TNF-R1, permitting the recruitment of proteins such as TRADD and TRAF2 to the active TNF-R1 signaling complex. SODD also interacted with death receptor–3 (DR3), another member of the TNF receptor superfamily. Thus, SODD association may be representative of a general mechanism for preventing spontaneous signaling by death domain–containing receptors.

TNF is a pleiotropic cytokine that signals through two distinct TNF receptors belonging to the rapidly expanding TNF receptor superfamily. Many of TNF's best characterized signaling pathways, such as induction of apoptosis and activation of the transcription factor NF-κB, are initiated by TNF-R1, whereas TNF-R2 appears to play a direct role in only a limited number of TNF responses (*1*). The intracellular portion of TNF-R1 contains a "death domain" of about 70 amino acids that is required for the signaling of apoptosis and NF-κB activation (*2*, *3*). Many

Tularik, Two Corporate Drive, South San Francisco, CA 94080, USA.

*To whom correspondence should be addressed. E-mail: goeddel@tularik.com

details of the molecular mechanisms of TNF-R1 signaling have been elucidated in recent years. In the initial step, TNF binds to the extracellular domain of TNF-R1 and induces receptor trimerization (*4*). Next, the aggregated death domain of TNF-R1 recruits the adapter protein TRADD (*3*). TRADD, in turn, recruits FADD, TRAF2, and RIP to form the TNF-R1 signaling complex and activate signaling cascades leading to apoptosis (*5*, *6*), JNK/SAPK activation (*5*, *7*), and NF-κB activation (*8*), respectively.

In addition to TNF-R1, several other members of the TNF receptor superfamily, including Fas, DR3, DR4, and DR5, contain intracellular death domains and are capable of triggering apoptosis when activated by their respective ligands (*9*). The death domains of these receptors can self-associate and bind other death domain–containing proteins, demonstrating that death domains function as protein-protein interaction domains (*3*, *10*). It has been exceedingly difficult to generate stable cell lines that overexpress death domain receptors (DDRs), presumably because overexpression leads to receptor aggregation and constitutive activation of the apoptotic machinery. Yet DDRs are naturally expressed in many tissues and cell lines, where they are maintained in an inactive state in the absence of their cognate ligands. These observations suggest the existence of a cellular mechanism that protects against ligand-independent signaling by TNF-R1 and other DDRs.

During the course of a search for DR3-interacting proteins (*11*), we isolated a cDNA clone encoding a 457–amino acid protein we have designated SODD for silencer of death domains (Fig. 1A). Northern (RNA) blot analysis showed that the ~3.5-kb SODD mRNA was expressed in all human tissues examined (Fig. 1B). Polyclonal antibodies raised against SODD recognized a protein doublet of about 60 kD in several human cell lines (Fig. 1C).

Additional yeast two-hybrid interaction assays showed that SODD associated with the intracellular domains of TNF-R1 and DR3 but not with those of TNF-R2, Fas, DR4, or DR5 (*12*). To confirm the interactions observed in yeast, we did coprecipitation assays in human embryonic kidney 293 cells (*13*). Glutathione S-transferase (GST) fusion proteins of the intracellular regions of various TNF receptor family members were transiently coexpressed with epitope-tagged SODD. Cell extracts were precipitated with glutathione agarose beads and analyzed for coprecipitating SODD by immunoblotting. In

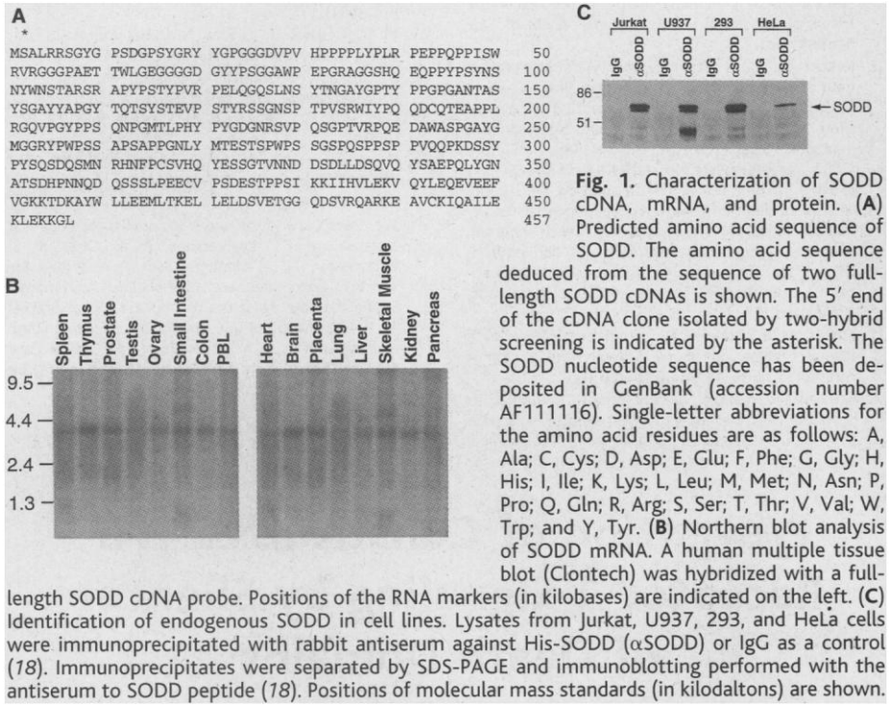

Fig. 1. Characterization of SODD cDNA, mRNA, and protein. (**A**) Predicted amino acid sequence of SODD. The amino acid sequence deduced from the sequence of two full-length SODD cDNAs is shown. The 5′ end of the cDNA clone isolated by two-hybrid screening is indicated by the asterisk. The SODD nucleotide sequence has been deposited in GenBank (accession number AF111116). Single-letter abbreviations for the amino acid residues are as follows: A, Ala; C, Cys; D, Asp; E, Glu; F, Phe; G, Gly; H, His; I, Ile; K, Lys; L, Leu; M, Met; N, Asn; P, Pro; Q, Gln; R, Arg; S, Ser; T, Thr; V, Val; W, Trp; and Y, Tyr. (**B**) Northern blot analysis of SODD mRNA. A human multiple tissue blot (Clontech) was hybridized with a full-length SODD cDNA probe. Positions of the RNA markers (in kilobases) are indicated on the left. (**C**) Identification of endogenous SODD in cell lines. Lysates from Jurkat, U937, 293, and HeLa cells were immunoprecipitated with rabbit antiserum against His-SODD (αSODD) or IgG as a control (*18*). Immunoprecipitates were separated by SDS-PAGE and immunoblotting performed with the antiserum to SODD peptide (*18*). Positions of molecular mass standards (in kilodaltons) are shown.

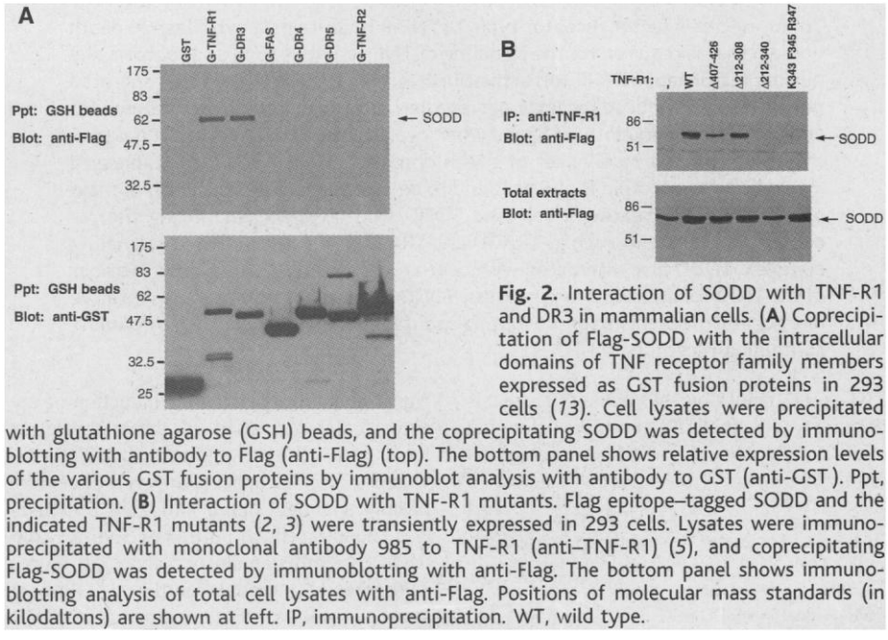

Fig. 2. Interaction of SODD with TNF-R1 and DR3 in mammalian cells. (**A**) Coprecipitation of Flag-SODD with the intracellular domains of TNF receptor family members expressed as GST fusion proteins in 293 cells (*13*). Cell lysates were precipitated with glutathione agarose (GSH) beads, and the coprecipitating SODD was detected by immunoblotting with antibody to Flag (anti-Flag) (top). The bottom panel shows relative expression levels of the various GST fusion proteins by immunoblot analysis with antibody to GST (anti-GST). Ppt, precipitation. (**B**) Interaction of SODD with TNF-R1 mutants. Flag epitope–tagged SODD and the indicated TNF-R1 mutants (*2*, *3*) were transiently expressed in 293 cells. Lysates were immunoprecipitated with monoclonal antibody 985 to TNF-R1 (anti–TNF-R1) (*5*), and coprecipitating Flag-SODD was detected by immunoblotting with anti-Flag. The bottom panel shows immunoblotting analysis of total cell lysates with anti-Flag. Positions of molecular mass standards (in kilodaltons) are shown at left. IP, immunoprecipitation. WT, wild type.

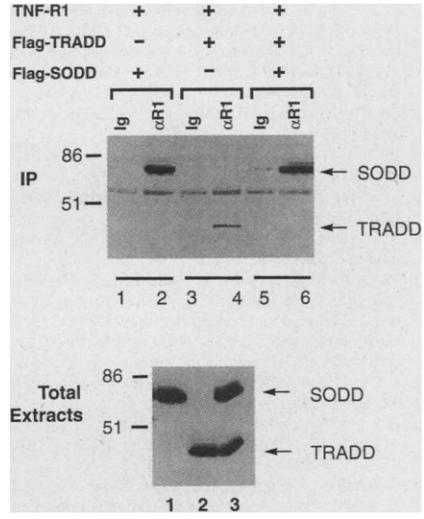

Fig. 3. SODD inhibits the interaction between TNF-R1 and TRADD. 293 cells were transfected with the indicated combinations of expression plasmids (4 μg each). Cell lysates were immunoprecipitated with control mouse IgG (Ig) or monoclonal antibody 985 to TNF-R1 (αR1). Coprecipitating SODD and TRADD were detected by immunoblotting with anti-Flag (top). Immunoblotting analysis of total cell lysates with anti-Flag is shown (bottom). Positions of molecular mass standards (in kilodaltons) are indicated.

this assay, SODD interacted specifically with the intracellular regions of TNF-R1 and DR3 but not with those of other DDRs or TNF-R2 (Fig. 2A), confirming what we observed in yeast. In similar experiments, SODD did not interact with the death domain–containing cytoplasmic proteins TRADD, FADD, or RIP (*12*).

Because the death domain is a common feature of the intracellular tails of TNF-R1 and DR3, the above results suggested that SODD might recognize these two DDRs specifically through this domain. To investigate this possibility, we examined the interactions between SODD and four different TNF-R1 mutants in mammalian cell coimmunoprecipitation assays. Two TNF-R1 mutants (Δ407-426 and Δ212-308) with largely intact death domains could coprecipitate SODD, whereas two TNF-R1 constructs having mutations within the death domain (Δ212-340 and K343 F345 R347) could not (Fig. 2B). Thus, SODD recognizes the death domain of TNF-R1.

The interaction profile displayed by TNF-R1 mutants for SODD is the same as observed earlier for the interaction between these mutants and the adapter protein TRADD (*3*). To determine whether SODD and TRADD recognize overlapping or independent binding sites in the TNF-R1 death domain, we performed additional coimmunoprecipitation experiments. TNF-R1 was coexpressed with epitope-tagged SODD in the presence or absence of TRADD. As expected, both SODD and TRADD coprecipitated with TNF-R1 when expressed individually (Fig. 3, lanes 2 and 4). However, when SODD and TRADD were coexpressed at roughly equivalent levels, the interaction between TRADD and TNF-R1 was substantially reduced (Fig. 3, lane 6), demonstrating that SODD and TRADD cannot simultaneously interact with TNF-R1.

Protein-protein interactions that occur when the proteins are artificially overexpressed may not exist or may be difficult to detect in untransfected cells. We therefore examined two human cell lines, U937 and Jurkat, to determine whether endogenous SODD and TNF-R1 interact under physiological conditions. Lysates prepared from cells treated for 5 min with TNF or left untreated were immunoprecipitated with a nonagonistic antibody to the extracellular domain of TNF-R1. Coprecipitating SODD was readily detected in untreated cell lysates but was barely visible in the TNF-treated samples (Fig. 4A). Thus, SODD and TNF-R1 are preassociated, and TNF-induced aggregation of TNF-R1 leads to the disruption of the SODD–TNF-R1 complex. In contrast, the TNF-R1 signal transducers TRADD and TRAF2 are not constitutively associated with TNF-R1 but are recruited to TNF-R1 only after TNF treatment (Fig. 4A) (*5*, *14*). A time course experiment shows that SODD was rapidly released from TNF-R1 after TNF treatment but began to reassociate after about 10 min (Fig. 4B).

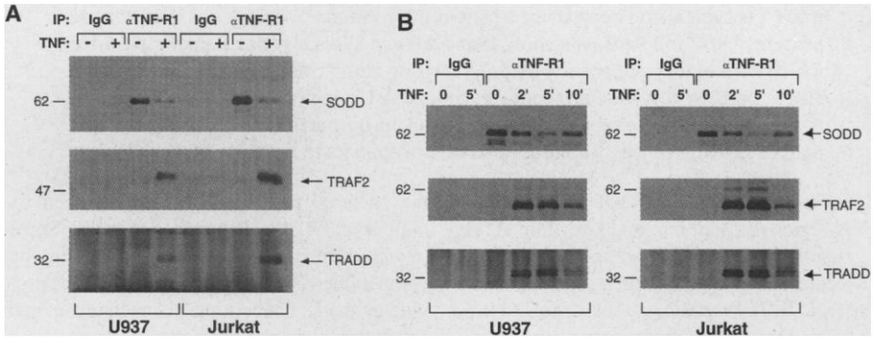

Fig. 4. TNF-dependent interaction of endogenous SODD and TNF-R1. **(A)** Release of SODD from TNF-R1 after TNF treatment. U937 or Jurkat cells (2×10^8) were treated with TNF (100 ng/ml) for 5 min or left untreated. Cell lysates were immunoprecipitated with monoclonal antibody 985 to TNF-R1 (αTNF-R1) or with control mouse IgG. Coprecipitating SODD, TRADD, and TRAF2 were detected by immunoblot analysis with antisera to SODD (*18*), TRADD (*5*), and TRAF2 (*14*), respectively. **(B)** Time course of SODD release from TNF-R1. For each lane, 2×10^8 cells were treated with TNF for indicated times and then processed as described for (A). Positions of molecular mass standards (in kilodaltons) are indicated.

Functional assays were performed to determine a possible role for SODD in TNF signaling. Overexpression of SODD in either 293 or HeLa cells failed to activate the well-characterized TNF-R1 cascades leading to apoptosis, NF-κB activation, or JNK activation (*12*). Moreover, SODD overexpression consistently suppressed the ability of TNF to activate an NF-κB–dependent reporter gene and inhibited TNF-induced cell death (Table 1). SODD overexpression also effectively inhibited NF-κB activation triggered by TNF-R1 overexpression (*12*). These results suggested that SODD may act as a silencer of TNF signaling. Therefore, we examined whether transient transfection of a SODD antisense vector in 293 cells might lead to ligand-independent signaling by TNF-R1. Expression of SODD antisense RNA gave only partial reduction in endogenous SODD levels (*12*) and resulted in minimal NF-κB activation in the absence of TNF (Table 1). However, cells expressing SODD antisense RNA demonstrated enhanced NF-κB activation and decreased viability after TNF treatment, results consistent with SODD being a negative regulator of TNF-R1 signaling.

The identification and characterization of SODD shed light on a previously unrecognized mechanism by which cells are able to carefully regulate signal transduction by TNF-R1 and other DDRs. The data presented above are consistent with a model in which SODD is a negative regulatory protein that is normally associated with the death domain of TNF-R1. SODD could inhibit the intrinsic self-aggregation properties of the death domain and maintain TNF-R1 in an inactive, monomeric state. This inhibition is relieved by TNF-mediated receptor cross linking, which triggers the rapid release of SODD from the death domain of TNF-R1. The uncomplexed death domains of TNF-R1 are then able to self-associate and bind the adapter protein TRADD, which in turn recruits TRAF2, RIP, and FADD to form an active TNF-R1 signaling complex. These signaling proteins begin to dissociate from the receptor within minutes of complex formation (Fig. 4B), in a process that is accompanied by the phosphorylation of TRADD (*15*). The subsequent reasso-

Table 1. Effects of altered SODD expression on NF-κB activation and cell viability. Human embryonic 293 cells were transfected by the calcium phosphate method (*3*) with a 3 μg of the empty vector pRK5, the SODD expression vector pRK-SODD, or the SODD antisense vector pRK-AS-SODD. All cells were also transfected with 1 μg of an E-selectin-luciferase reporter gene and 0.5 μg of the β-galactosidase expression vector pRSV–β-galactosidase (*19*). After 24 hours, cells were treated with TNF (20 ng/ml) for 6 hours or left untreated. Luciferase activity was measured and normalized for β-galactosidase expression as described (*19*) and are represented as the mean ± SD of four replicate samples. Mean cell viability (±SD of quadruplicate samples) after the TNF treatment was determined as described (*3*) and is shown relative to the viability of pRK-SODD–transfected cells.

Vector	NF-κB activation (relative luciferase activity)			Relative cell viability (%) (+TNF)
	−TNF	+TNF	Fold activation	
pRK5	1.0 ± 0.04	6.9 ± 1.2	6.9	49 ± 3
pRK-SODD	0.20 ± 0.01	0.48 ± 0.04	2.4	100 ± 30
pRK-AS-SODD	1.2 ± 0.2	15.8 ± 5.7	13.6	29 ± 10

ciation of SODD with the uncomplexed TNF-R1 then reestablishes the normal silent state for TNF-R1. This tight control of the duration of TNF signaling at the receptor level is somewhat analogous to the temporal regulation of NF-κB activity by the NF-κB inhibitor IκB that occurs downstream in the TNF signaling cascade. In addition to its role as a silencer of TNF-R1 signaling, we have considered the possibility that SODD may also participate in transducing TNF signals once it is released from the activated receptor complex. However, at this time, we have no evidence for such a signaling role.

It is likely that SODD also functions as an inhibitor of constitutive DR3 signaling because (i) SODD interacts with DR3 and TNF-R1 equally well in yeast two-hybrid and mammalian coprecipitation assays; (ii) DR3, like TNF-R1, signals independently of ligand when overexpressed (*16*); (iii) the death domains of DR3 and TNF-R1 are highly related, sharing 45% sequence identity; and (iv) TNF-R1 and DR3 both use TRADD, TRAF2, RIP, and FADD for signal transduction (*16*). Finally, on the basis of these results, we predict that SODD-related proteins will be found that interact with and play a similar role in preventing spontaneous signaling by Fas, DR4, and DR5. In fact, a candidate protein having 61% identity to the COOH-terminal 71 amino acids of SODD is predicted to be encoded by expressed sequence tag cDNA clones (*17*) found in the National Center for Biotechnology Information DNA database.

References and Notes

1. L. A. Tartaglia and D. V. Goeddel, *Immunol. Today* **13**, 151 (1992); P. Vandenabeele, W. Declercq, R. Beyaert, W. Fiers, *Trends Cell Biol.* **5**, 392 (1995).
2. L. A. Tartaglia, T. M. Ayres, G. H. W. Wong, D. V. Goeddel, *Cell* **74**, 845 (1993).
3. H. Hsu, J. Xiong, D. V. Goeddel, *ibid.* **81**, 495 (1995).
4. D. W. Banner *et al.*, *ibid.* **73**, 431 (1993).
5. H. Hsu, H.-B. Shu, M.-P. Pan, D. V. Goeddel, *ibid.* **84**, 299 (1996).
6. W.-C. Yeh *et al.*, *Science* **279**, 1954 (1998).
7. Z. Liu, H. Hsu, D. V. Goeddel, M. Karin, *Cell* **87**, 565 (1996); W.-C. Yeh *et al.*, *Immunity* **7**, 715 (1997).
8. H. Hsu, J. Huang, H.-B. Shu, V. Baichwal, D. V. Goeddel, *Immunity* **4**, 387 (1996); M. A. Kelliher *et al.*, *ibid.* **8**, 297 (1998).
9. A. Ashkenazi and V. M. Dixit, *Science* **281**, 1305 (1998).
10. H. Y. Song, J. D. Dunbar, D. B. Donner, *J. Biol. Chem.* **269**, 22492 (1994); M. P. Bolden *et al.*, *ibid.* **270**, 387 (1995).
11. The plasmid Gal4BD-DR3, which encodes the GAL4 DNA-binding domain fused to the intracellular domain (amino acids 227 to 418) of DR3, was used as bait in a yeast two-hybrid screen of a HeLa cell cDNA library (Clontech). The isolated positive clones were analyzed as described (*3*). Full-length SODD cDNA was obtained by screening a λZAP human Jurkat T cell cDNA library by standard methods (*3*).
12. Y. Jiang, W. Liu, D. V. Goeddel, unpublished data.
13. For protein-protein interaction assays, subconfluent 10-cm dish cultures of 293 cells were transfected by the calcium phosphate method (*3*). To determine SODD interaction with DDRs, we used expression vectors encoding Flag-SODD and GST-DDRs or GST. Twenty-four hours after transfection, cells were washed in phosphate-buffered saline and lysed in E1A lysis buffer (*3*). Lysates were precipitated with glutathione agarose beads (Pharmacia Biotechnology), and the beads were washed three times with E1A buffer and twice with E1A buffer containing 1 M NaCl. The precipitates were fractionated on SDS–polyacrylamide gel electrophoresis (SDS-PAGE) and transferred to a nitrocellulose membrane. The coprecipitated SODD was detected by immunoblot analysis with polyclonal antibodies to the Flag epitope (Santa Cruz Biotechnology). To determine SODD binding to various TNF-R1 mutants (*2*, *3*), we incubated cell lysates for 2 to 4 hours at 4°C with monoclonal antibody 985 to TNFR1 (*5*) or control mouse immunoglobulin G (IgG) monoclonal antibody (Sigma) and 25 μl of 1:1 slurry of protein G–Sepharose (Pharmacia). Beads were washed twice with 1 ml of E1A buffer, twice with 1 ml of high salt E1A buffer, and twice again with E1A buffer before immunoblot analysis was performed.
14. H.-B. Shu, M. Takeuchi, D. V. Goeddel, *Proc. Natl. Acad. Sci. U.S.A.* **93**, 13973 (1996).
15. M. Tanaka and D. V. Goeddel, unpublished data.
16. A. M. Chinnaiyan *et al.*, *Science* **274**, 990 (1996); J. Kitson *et al.*, *Nature* **384**, 372 (1996); S. Marsters *et al.*, *Curr. Biol.* **6**, 1669 (1996).
17. GenBank accession numbers AA319013, AA362082, H10621, and T33545.
18. Rabbit polyclonal antisera were generated against a SODD peptide (amino acids 292 to 313) and against purified His-tagged SODD produced in *Escherichia coli*. The upper band of the protein doublet in Fig. 1C is presumably phosphorylated SODD. This band predominates in cell lines that express low levels of SODD, whereas both bands are apparent in cell lines that express higher levels (*12*).
19. J. D. Woronicz, X. Gao, Z. Cao, M. Rothe, D. V. Goeddel, *Science* **278**, 866 (1997).

20. We thank L. Huang for synthesizing the SODD peptide for antibody generation, V. Dixit for providing the DR3 cDNA, A. Ashkenazi for providing DR4 and DR5 cDNAs, D. Baltimore for supplying the parental mammalian cell expression vector for GST, pEBG, and L. Medin for help with the figures.

9 October 1998; accepted 21 December 1998

Silencing of Genes Flanking the P1 Plasmid Centromere

Oleg Rodionov, Małgorzata Łobocka,* Michael Yarmolinsky†

Partition modules stabilize bacterial plasmids and chromosomes by actively promoting their segregation into daughter cells. The partition module of plasmid P1 is typical and consists of a centromere site, *parS*, and genes that encode proteins ParA and ParB. We show that ParB can silence genes flanking *parS* (to which ParB binds), apparently by polymerizing along the DNA from a nucleation site at *parS*. Wild-type ParB contacts an extensive region of P1 DNA; silencing-defective ParB proteins, which were found to be partition-defective, are less able to spread. Hence, the silenced structure appears to function in partitioning.

In eukaryotes, transcriptional silencing of DNA regions, which range in size from short segments to entire chromosomes, is an essential feature of development (*1*). In fission yeast and in *Drosophila*, extensive regions of silencing that spread from centromeric sites appear to be necessary for full centromere functioning (*2*). We consider the possibility that silencing may have a role in the prokaryotic equivalent of mitosis—the process of partitioning plasmids and chromosomes (ensuring their orderly segregation to daughter cells). Knowledge of partitioning has been mainly derived from studies of plasmid-encoded partitioning genes and their chromosomal homologs, which have been recognized to be present in diverse bacteria (*3–5*). Although the few reports of silencing in bacteria are generally of silencing over short regions, studies have shown that genes several kilobases distant from the centromere of the bacterial plasmid F can be silenced by high levels of the F partition protein, SopB (*6, 7*). Here, we characterize silencing by comparable elements of the P1 plasmid, provide evidence concerning its mechanism, and assess its relevance for partitioning.

P1 partitioning requires two P1 proteins (ParA and ParB) and a DNA site (*parS*) (*8*). ParB binds to *parS* (*9, 10*); ParA is an adenosine triphosphatase (*11*). These factors, together with unknown host components, ensure plasmid stability. We previously observed that, dependent on the location of *parS*, ParB can either destabilize a *parS*-bearing plasmid (*12*) or prevent such a plasmid from conferring antibiotic resistance (*13*), perhaps by gene silencing in each case. To further study silencing, we inserted *parS* and reporter genes *lacZ* and *cat* at the λ attachment site (*att*λ) of *Escherichia coli*, close to the biotin biosynthesis genes (*bioA*, *B*, *F*, *C*, and *D*) (Fig. 1A). We made constructs with *parS* in opposite orientations (I and II) and a construct without *parS* (0). ParB was supplied from an inducible plasmid source.

Expression of the *cat*, *lacZ*, and *bio* genes was markedly decreased by the presence of wild-type ParB, in contrast to their expression in controls that lacked *parS* or in which

Laboratory of Biochemistry, National Cancer Institute, 37 Convent Drive, Bethesda, MD 20892–4255, USA.

*Present address: Department of Microbial Biochemistry, Institute of Biochemistry and Biophysics, Polish Academy of Sciences, ul. Pawińskiego 5A, 02-106, Warsaw, Poland.

†To whom correspondence should be addressed. E-mail: myarmo@helix.nih.gov